Laser and Particle Beams (2013), *31*, 597–605.

doi:10.1017/S0263034613000517

Influence of the initial size of the proton layer in sheath field proton acceleration

JINQING YU,[1,2,3] XIAOLIN JIN,[1] WEIMIN ZHOU,[2] BO ZHANG,[2] ZONGQING ZHAO,[2] LEIFENG CAO,[2] BIN LI,[1] YUQIU GU,[2,4] RONGXIN ZHAN,[5] AND Z. NAJMUDIN[3]

[1]Vacuum Electronics National Laboratory, University of Electronic Science and Technology of China, Chengdu, People's Republic of China
[2]Science and Technology on Plasma Physics Laboratory, Research Center of Laser Fusion, China Academy of Engineering Physics, Mianyang, People's Republic of China
[3]The Blackett Laboratory, Imperial College, London, United Kingdom
[4]Institute of Engineering Physics, College of Science National University of Defense Technology, Changsha, People's Republic of China
[5]School of Information Engineering, Zhengzhou University, Zhengzhou, People's Republic of China

(RECEIVED 25 April 2013; ACCEPTED 4 May 2013)

Abstract

We investigate the influence of the initial size of the proton layer on proton acceleration in the interaction of high intensity laser pulses with double-layer targets by using two-dimensional particle-in-cell code. We discuss the influence of proton layer initial sizes on the cut-off energy, energy spread, and divergence angle of proton beam. It is found that Coulomb explosion plays an important role on the proton cut-off energy. This causes the cut-off energy to increase for increasing proton layer thickness, at the expense of energy spread. The proton divergence angle reaches a peak value and then falls again with increasing the width. Proton divergence angle grows with target thickness. It is found that there is an optimal thickness to obtain the narrowest energy spread, which may provide an effective method (change the size of proton layer) to obtain high quality proton beams. This work may serve to improve the understanding of sheath field proton acceleration.

Keywords: Coulomb explosion; Initial size of the proton layer; Particle-in-cell; Sheath field proton acceleration

1. INTRODUCTION

In the past 20 years, as the developments of ultra-high power and ultra-short pulse lasers, laser-plasma interaction (LPI) (Cai *et al.*, 2009; Pukhov *et al.*, 2011; Robinson *et al.*, 2012; Sakagami *et al.*, 2012) has attracted remarkable interests in relativistic plasma physics. One of the hottest topics in the field of LPI is laser-driven ion (proton) acceleration (Eliasson *et al.*, 2009; Pae *et al.*, 2011) because of its potential applications in high energy density physics diagnostics (Li *et al.*, 2006; 2009), fast ignition in inertial confinement fusion (Roth *et al.*, 2001; Badziak *et al.*, 2011), and hadron therapy (Malka *et al.*, 2004). When an ultra-intense laser pulse irradiates on a solid target, relativistic electrons generates at the interface. The relativistic electrons moving through the plasma-vacuum interface create a space charge field on the target rear side, and the strong perpendicular electrostatic field accelerates protons to high energies: this mechanism is known as "target normal sheath acceleration" (TNSA) (Wilks *et al.*, 2001) mechanism. TNSA is one of the major mechanisms in laser proton acceleration and considered to be an effective method to obtain high quality proton beams with the laser systems nowadays.

Although there were a lot of theoretical (Mora, 2005; Passoni & Lontano, 2008; Fourkal *et al.*, 2005; Passoni *et al.*, 2010), experimental (Schwoerer *et al.*, 2006; Hegelich *et al.*, 2006; Ter-Avetisyan *et al.*, 2009; Bartal *et al.*, 2011; Brenner *et al.*, 2011; Burza *et al.*, 2011), and simulation (Nodera *et al.*, 2008; Klimo *et al.*, 2011; Lefebvre *et al.*, 2010) studies that have been reported to enhance our understanding of TNSA mechanism and improve proton beam quality, there still are numerous issues to overcome as the present proton beam sources are not yet optimized for applications. In potential applications of proton beam, proton cut-off energy, proton energy spread ($\Delta E/E_{FWHM}$) and proton divergence angle (Andreev *et al.*, 2010) are all

Address correspondence and reprint requests to: Bin Li, Vacuum Electronics National Laboratory, University of Electronic Science and Technology of China, Chengdu 610054, People's Republic of China. E-mail: libin@uestc.edu.cn

important parameters (Daido *et al.*, 2012), These are affected by a number of parameters, such as the characteristics of the laser pulse, and the parameters of the foil target and proton layer. The dependence of proton acceleration on the laser pulse (Zeil *et al.*, 2010; Carrié *et al.*, 2009; Esirkepov *et al.*, 2006) and the foil target size have been investigated in detail. However, there have been a few considerations the influence of the proton layer (Flacco *et al.*, 2010). The influence of the proton layer can also help probe diagnose the sheath acceleration mechanism leading to generation of proton beam. Changing the transverse size of the deposited proton layer, it is possible to create for the protons a region in space where the accelerating electric field is homogeneous and constant. If all the protons are accelerated in the same fashion, their energy will tend to be the same creating a peak in the energy spectrum. Meanwhile, changing the longitudinal size proton layer, both of proton bunch Coulomb explosion effect and screening on sheath field will affect the acceleration.

In this work, we adopt a double-layer target composed of a high-Z foil layer and a proton layer. The radio me/mp of proton is larger than that of high-Z ion, so as to achieve high efficient acceleration. The high-Z substrate having a plasma frequency smaller than the proton layer will start expanding under the influence of the ambipolar field after the proton layer is accelerated. The dynamic of the substrate is decoupled from the dynamic of the proton layer. We change the proton layer size and carry out simulations with relativistic two-dimensional particle-in-cell (2D-PIC) code (collisionless) Flips2d (Zhou *et al.*, 2010; Yu *et al.*, 2012*a*; 2012*b*; 2013). PIC simulation is probably the most successful method for investigating laser driven proton acceleration. Compared with three-dimensional (3D)-PIC simulations, 2D simulations have their limitations in providing quantitative comparisons, but they do provide useful qualitative guides for experiments. We organize this paper as follows, the setup of the PIC simulations is described in Section 2, the influence of the proton layer width (in the transverse direction) and thickness (in the longitudinal or laser incident direction) are presented in Sections 3 and 4, respectively, and a summary is given in Section 5.

2. SIMULATION CONDITIONS

We choose a simulation box sized $X_L \times Y_L = 50\ \lambda_0 \times 80\ \lambda_0$, simulation duration of $250\,\tau$, and grid size of $\Delta X = \Delta Y = 0.02\ \lambda_0$ and time step of $\Delta t = 0.01\,\tau$, where $\tau = \lambda_0/c \approx 3.536\,fs$ and $\lambda_0 = 1.06\ \mu m$ are laser period and wavelength, respectively. A p-polarized laser pulse with Gaussian profile in the transverse direction and focal spot of $3.5\ \lambda_0$ (full-width half maximum (FWHM)) is introduced along the laser-axis from the left. In longitudinal direction, the pulse shape is assumed to increase to peak intensity in $5\,\tau$, then remain constant for $30\,\tau$ before dropping to zero in another $5\,\tau$. The dimensionless amplitude is assumed to be $a_0 = 10.0$, where a_0 is the normalized field amplitude. The electron and ion initial temperatures are both 1.0 keV. We use a double-layer target model (Reference 37) in the simulations. A high-Z ($Zme/mi = 1/3672$) thin foil target of $1.0\ \lambda_0$ thickness and $10.0\ \lambda_0$ wide is used as shown in Figure 1. A hydrogen layer ($me/mp = 1/1836$) is attached to the rear of the high-Z foil target. The density of the high-Z foil is $50n_c$, where $n_c \approx 1.0 \times 10^{21}/cm^3$ is the critical density. The density of the hydrogen layer is n_c . The number of particles per cell is 225 electrons and 25 ions for the high-Z foil target, 225 electrons and 225 protons for the hydrogen layer. In order to improve the computational precision, a second-order interpolation algorithm for charge conservation of PIC method (Yu *et al.*, 2013) has been adopted in the code. The boundary conditions of fields are absorption in transverse direction and periodic in longitudinal direction, while the conditions of particles are absorption and reemission. The parameters used in this paper may be not justified; especially the optimal target condition is not addressed here, as this paper's focus is on the TNSA physics.

3. EFFECT OF PROTON LAYER WIDTH

In this section, we discuss the simulation results where the transverse width of the proton layer width from $0.1\ \lambda_0$ to $10\,\lambda_0$, while keeping the thickness fixed to $0.1\,\lambda_0$. In the work of Fuchs *et al.* (2006), it is shown that the effective acceleration time is proportional to laser pulse duration, as $t_{acc} \approx 1.3 t_{Laser}$, where t_{acc} is the effective acceleration time and t_{Laser} is laser pulse duration. In our simulations, the effective acceleration time should be about $50\,\tau$ (our laser duration full-width half maximum is $t_{Laser} \approx 35\,\tau$), which means that the acceleration process in sheath field is finished at the end of simulation time ($250\,\tau$). The proton energy spectra generated from proton layers of different width at $t = 250\,\tau$ is shown in Figure 2a, the spectra shape is significantly affected by the width of the proton layer. In these results, the average proton energy decreases as the transverse width

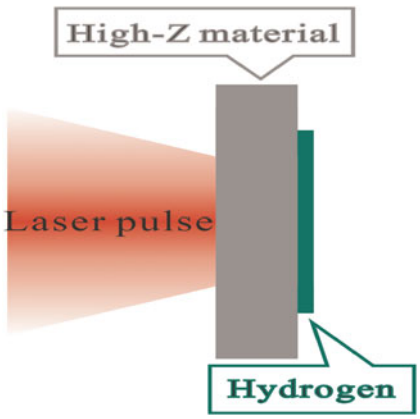

Fig. 1. (Color online) A laser pulse is irradiated on a high-Z foil target from the left. The thickness, width and density of the foil target are $1.0\ \lambda_0$, $10.0\ \lambda_0$ and $50n_c$, respectively. A hydrogen layer is attached to the rear of the high-Z foil. The density of the hydrogen layer is $1.0n_c$

https://doi.org/10.1017/S0263034613000517 Published online by Cambridge University Press

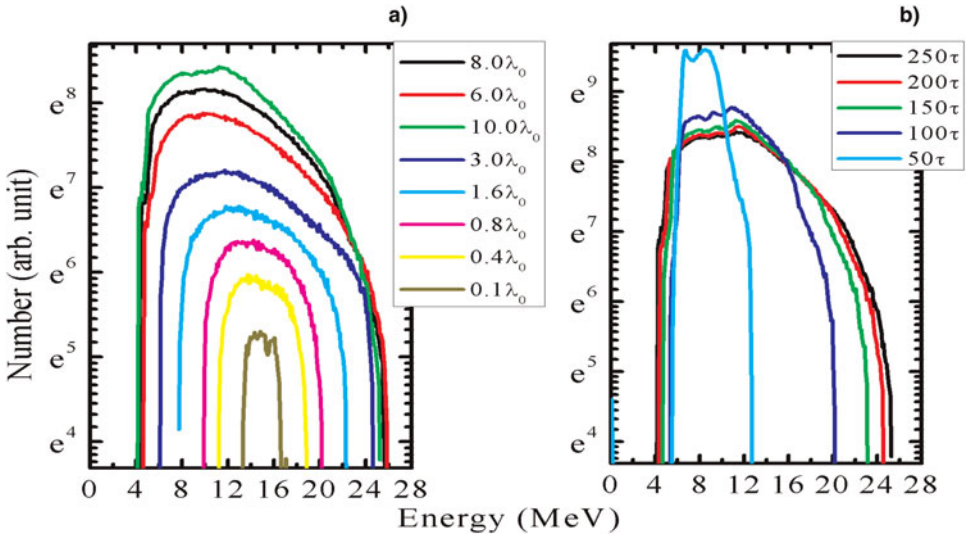

Fig. 2. (Color online) (**a**) Proton energy spectra for different proton layer width (transverse size) at $t = 250\ \tau$, from which time the effect of sheath field acceleration is finished for the width of proton layer from $0.1\ \lambda_0$ to $10\ \lambda_0$ and constant the thickness $0.1\ \lambda_0$, (**b**) Proton energy spectrum of proton layer with $10\ \lambda_0$ wide at different times. We can see the expansion of the bandwidth of the energy spectrum after the acceleration process.

increases, because protons far from the laser axis acquire a lower energy as shown in Figure 3. The proton cut-off energy however increases as the width grows from $0.1\ \lambda_0$ to $6.0\ \lambda_0$, and then slightly decreases as shown in Figure 2a. The reason for such a trend is that the proton cut-off energy is affected by both sheath field value and the internal Coulomb explosion of the proton beams, which is investigated in detail below. The proton energy spectrum of a $10\ \lambda_0$ wide layer is shown at different times in Figure 2b. One can see that the proton energy spectrum has a sharp peak at early time, expands with time in spite of the fact that we expect the sheath acceleration to have finished,

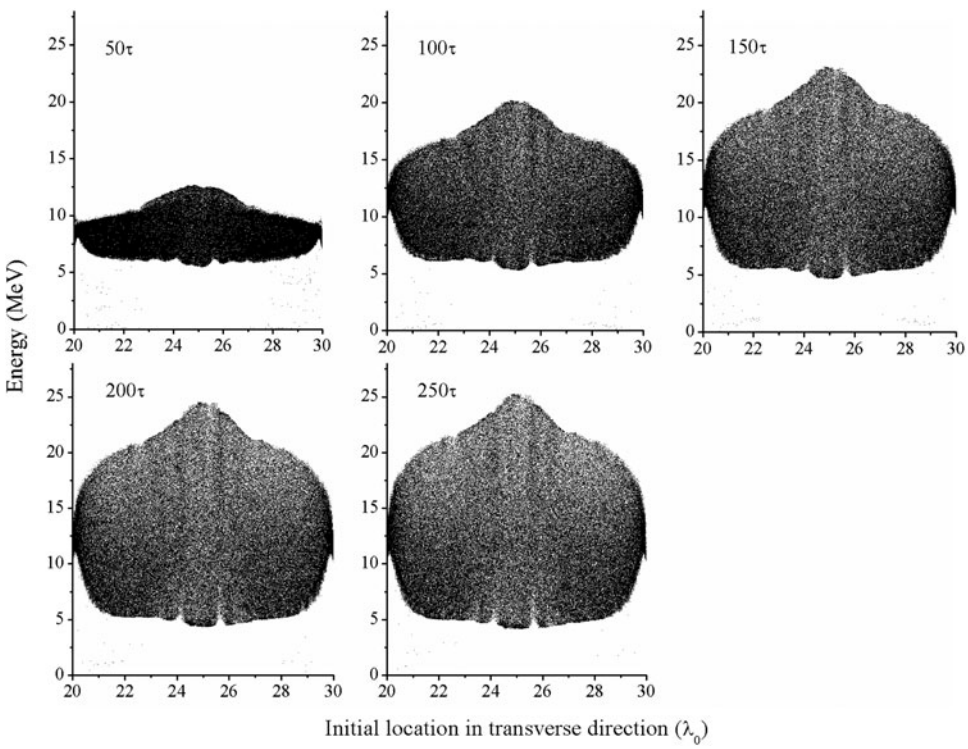

Fig. 3. Relations between proton energy and their initial locations in transverse direction at different times for a proton layer $10\ \lambda_0$ wide and $0.2\ \lambda_0$ thick.

https://doi.org/10.1017/S0263034613000517 Published online by Cambridge University Press

which is due to the Coulomb explosion effect as mentioned above.

Figure 3 shows the relation between proton energies and their initial locations in transverse direction at different times. This figure gives two pieces of information. The first one is that the proton energy range varies significantly after the acceleration. This result (and also the result shown in Fig. 2b) indicates that Coulomb explosion plays a very important role in expansion of proton energy spectrum. The second one is that protons with higher energy are originally located near the laser axis. The reason is that E_x, the sheath electric field on the rear of the foil target is stronger near laser axis, because the laser field is strongest there, and thus generates a relativistic electron beam that of high energy on laser axis. Furthermore, the energies of all protons are above 5MeV can be seen from the picture. That is because in this work, we adopt a double-layer target (Esirkepov *et al.*, 2002) with different ratio of Zme/mi, and the proton layer with a larger ratio than high-Z layer can obtain more efficiency acceleration.

In proton acceleration, proton cut-off energy, proton energy spread, and divergence angle are important parameters to judge the quality of proton beams. From the spectra shown in Figure 2a, we obtain the proton cut-off energy (black curve with squares) and energy spreads (blue curve with squares) for different width of the proton layer as shown in Figure 4a. In order to explain the trends of proton cut-off energy, energy spread, and expansion of energy spectra, we introduce a proton beam Coulomb explosion model during acceleration. The Coulomb explosion should be considered in all directions. For convenience, we divide the Coulomb explosion process into transverse and longitudinal directions, respectively. In the transverse direction, the Coulomb explosion can be assumed to be symmetric around the laser axis, because the sheath field in the transverse direction can be considered to be symmetric along the laser axis. We also assume that all of the electrons escape from the proton layer. Based on these two assumptions, the maximum electric field located at the top or bottom sides of the proton beam can be expressed as

$$\vec{E}_{in}\left(\frac{w}{2}, t\right) = \vec{E}_{SW} + 2\pi e n_0 w \cdot \vec{n}, \tag{1}$$

where $\vec{E}_{SW}$ is the sheath field (in longitudinal direction) experienced on proton, which depends on the top (bottom) protons locations, $2\pi e n_0 w \cdot \vec{n}$ (Fourkal *et al.*, 2005; Zhang *et al.*, 2009) is the transverse field experienced on proton from Coulomb explosion effect, where w denotes the width of proton layer, and n_0 is proton layer's density. $\vec{n}$ is a unit vector in transverse direction. From Eq. (1), one can see that the maximum electric field due to the Coulomb explosion of the proton beam is proportional to the width and density of the proton layer. In the case of $w = 0.1\,\lambda_0$ (i.e., the number of protons is very small), the Coulomb explosion effect of the protons is weak and the acceleration can be considered to be dominated by the sheath field. Increasing the width of the proton layer from $0.1\,\lambda_0$ to $6.0\,\lambda_0$ (the proton number increases), the Coulomb explosion effect on the top (bottom) protons increases significantly, while the effect of sheath field near the laser axis can be considered to be constant because the size of proton layer is fixed in the longitudinal direction. This is why the proton cut-off energy increases with the proton width as shown in Figure 4a (black curve with squares). For Further increase, the transverse size (from $6.0\,\lambda_0$ to $8.0\,\lambda_0$), although the Coulomb explosion effect on the top (bottom) protons increases, the sheath field experience on these proton become very weak (the sheath electric field on the rear of the foil target is

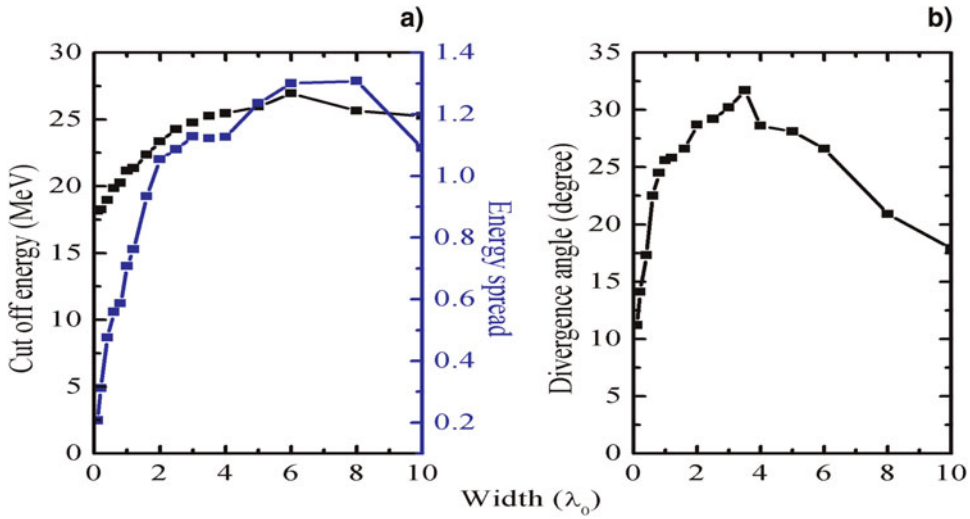

Fig. 4. (Color online) (**a**) Proton energy spread (blue curve with squares) and proton cut-off energy (black curve with squares) for different proton layer transverse width (the thickness is fixed to $0.1\,\lambda_0$) at the time of $250\,\tau$. (**b**) Proton divergence angles from different proton layer width at the time of $250\,\tau$.

https://doi.org/10.1017/S0263034613000517 Published online by Cambridge University Press

stronger near laser axis as discussed above). For this reason, the proton cut-off energy reduces slightly with further increase of the width as shown in Figure 4a (black curve with squares). This along with the reduced Coulomb explosion means that the energy spread becomes narrower with reduced proton layer width as shown in Figure 4a (blue curve with squares). The trend of energy spread is accordance the experiment results obtained by using small sized proton layer (Pfotenhauer *et al.*, 2008).

Figure 4b shows the proton beam divergence angle at $t = 250\,\tau$ again as a function of proton layer transverse width. The proton divergence angle reaches a peak value near 4.0 λ_0 (this value is also influenced by the high-Z layer, proton layer parameters and laser conditions, which will be investigated in the future). To investigate the trend of proton divergence angle shown in Figure 4b, we investigate the relation between proton emergence angle and the initial locations for different proton layer widths as shown in Figure 5. The emergence angle is $\theta = \arctan(v_y/v_x)$, where v_y and v_x are proton velocities in transverse and longitudinal directions, respectively. From the figure, one can see the following. First, the emergence angle of a proton depends on its initial transverse location. Protons with large emergence angle come from locations far away from the laser axis. (further reasons for this trend can be considered to be proton emergence angle related to proton energy, which is discussed below). The outermost (in transverse direction) protons receive the largest emergence angles. Second, the peak emergence angle increases with the proton layer width because Coulomb explosion effect increases with the width. Meanwhile, the outermost protons compress the inner ones and this compressing force also increases with proton width, therefore, the largest emergence angle does not increase linearly with proton layer width and the divergence angle decreases when the proton width changes from 4.0 λ_0 to 10.0 λ_0 as shown in Figure 4b.

4. EFFECT OF PROTON LAYER THICKNESS

In this section, we discuss results for different proton layer thickness from 0.04 λ_0 to 1.0 λ_0, while the transverse width is fixed at 5.0 λ_0. The proton energy spectra at $t = 250\,\tau$ are shown in Figure 6. One can see that the average proton energy decreases with increasing thickness due to the much larger layer thickness. Meanwhile, the maximum and minimum proton energies are affected by the thickness significantly.

From the spectra in Figure 6, we obtain the cut-off energy and the energy spread for different proton layer thickness in Figure 7a. In considering proton energy spread (blue curve with squares), one can see that there is an optimal thickness for proton acceleration. This optimal thickness may be influenced by the laser condition, initial density of proton layer, and foil target. This result also indicates that optimization of the proton layer thickness provides an effective way to obtain high quality proton beams of narrow energy spread. In order to explain the trend of proton cut-off energy shown in Figure 7a (black curve with squares), we introduce a longitudinal (direction of laser incidence) proton beam Coulomb explosion model. We introduce a moving reference frame for the proton beam, in which the Coulomb explosion can be assumed to be quasi-symmetric. The velocity of the moving reference frame varies with time, which is determined by the sheath field. The maximum electric field in the longitudinal direction located at the front of the proton beam can be expressed by an equation similar to Eq. (1)

$$E_{in}\left(\frac{l}{2}, t\right) = E_{SL} \pm \frac{2\pi e n_0 l}{1 + 2\pi n_0 e^2 t^2/m_p}, \tag{2}$$

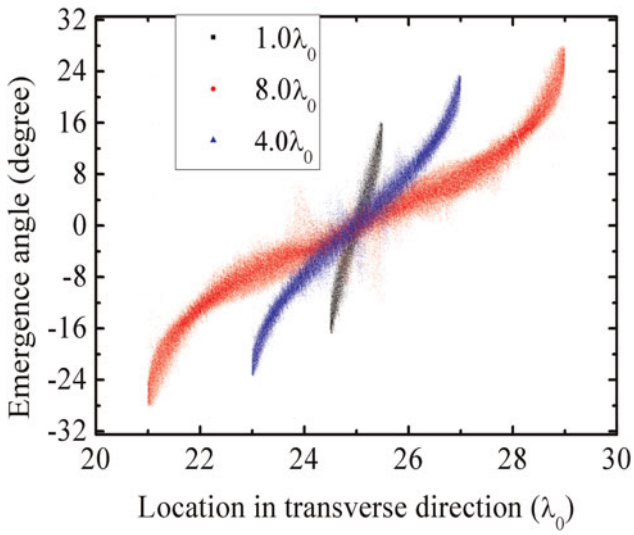

Fig. 5. (Color online) The relation between proton emergence angle and their initial locations at $t = 250\,\tau$ for an initial proton layer transverse widths of 1.0 λ_0, 4.0 λ_0, 8.0 λ_0.

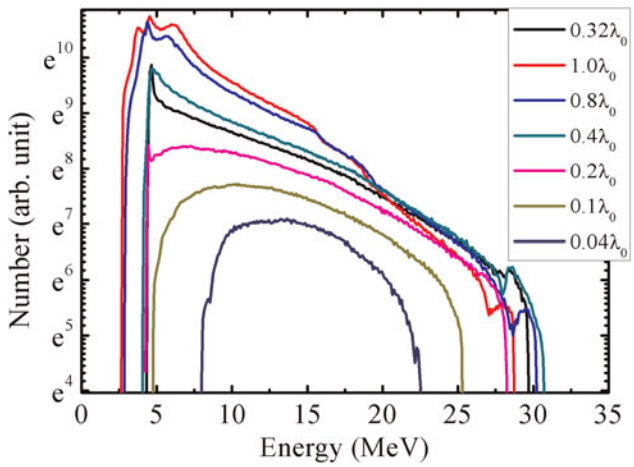

Fig. 6. (Color online) Proton energy spectra for different proton layer thickness at the time of 250 τ, the thickness is changed from 0.04 λ_0 to 1.0 λ_0 and the transverse width is fixed to 5.0 λ_0.

https://doi.org/10.1017/S0263034613000517 Published online by Cambridge University Press

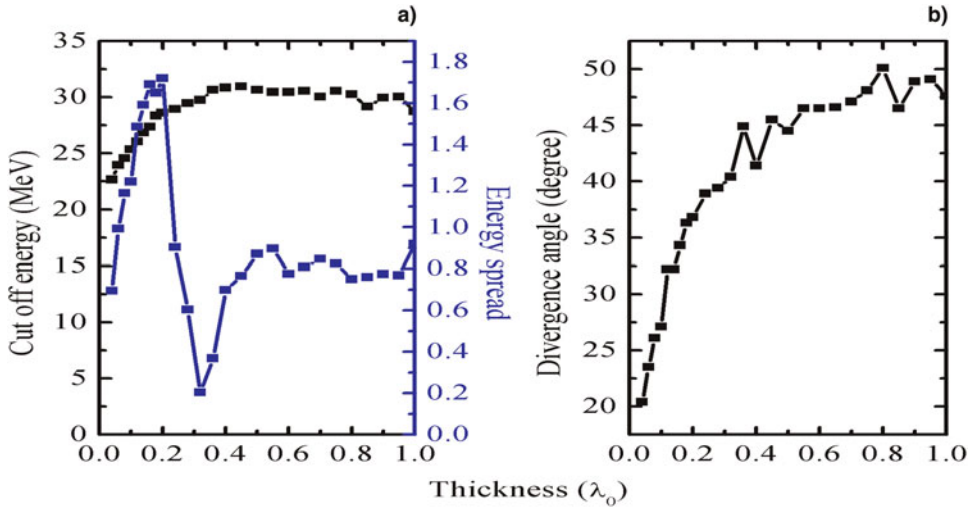

Fig. 7. (Color online) (**a**) Proton energy spread (blue curve with squares) and cut-off energy (black curve with squares) for different proton layer thickness at $t = 250\ \tau$, (**b**) Proton divergence angles from varies proton layer thickness at $t = 250\ \tau$, the proton layer transverse width is fixed at $5.0\ \lambda_0$.

where E_{SL} is the sheath field on the laser axis experienced on proton, the other part of right-hand in Eq. (2) is the electric field from Coulomb explosion (Fourkal *et al.*, 2005; Zhang *et al.*, 2009) (this field is in longitudinal direction), $1/2$ and m_p denote the coordinate of the proton front in the moving reference frame and the proton mass, respectively. From Eq. (2), one can see that the maximum electric field due to the Coulomb explosion is proportional to the thickness and density of the proton layer. From Figure 7a (black curve with squares), one can see that the proton cut-off energy increases with thickness from $0.04\ \lambda_0$ to $0.45\ \lambda_0$, and then decreases when the thickness is above $0.45\ \lambda_0$. For thickness up to $0.45\ \lambda_0$, the energy due to acceleration from sheath field is almost the same, but the effect of Coulomb explosion increases significantly, which means that the proton cut-off energy is enhanced as the thickness is increased. For further increase proton layer thickness from $0.45\ \lambda_0$ to $1.0\ \lambda_0$, although the Coulomb explosion effect continues to increase, the screening of the sheath field by the proton layer is also enhanced. This is the reason why the cut-off energy reduces for thickness greater than $0.45\ \lambda_0$ as shown in Figure 7a (black curve with squares).

Figure 7b shows the proton divergence angle (full-width half maximum (FWHM)) for different proton layer thickness. From this figure, one can see that the proton divergence angle grows with the thickness. To investigate the mechanism for the proton divergence angle trend shown in Figure 7b, the relation between proton energy and initial longitudinal proton locations is shown in Figure 8. This gives three pieces of information. The first is that the proton cut-off energy and minimum proton energy vary with thickness, determined by both the sheath field and the Coulomb explosion effect. The results are consistent with the spectra shown in figure 6. The second is that the protons with higher energy are initially located at both the front and the rear of proton layer. Higher energy protons are only accelerated from the front of proton layer for ultra-thin proton layer such as for $0.04\ \lambda_0$). The third piece of information is that lower energy protons are accelerated from the middle of the proton layer.

In the work of Andreev *et al.* (2010), it was found that the proton emergence angle depends on its energy and position, and that protons with higher energy tend to have smaller emergence angle. As we have found in Figures 6 and 8, the minimum proton energy decreases with increasing proton layer thickness. Figure 9 shows protons with larger emergence angle also come from middle of the proton layer, and the largest emergence angle grows with thickness. The results shown in Figures 8 and 9 (also Figs. 3 and 5) are consistent with the results from the model and simulations of Andreev *et al.* (2010). Meanwhile the results in Figures 8 and 9 also explain why the divergence angle grows with the thickness as shown in Figure 7b.

5. CONCLUSION

We have studied the interactions of intensity laser pulse with double-layer foil targets by 2D-PIC simulation. We focus on the influence of the initial size of the proton layer on the proton cut-off energy, energy spread and divergence angle in sheath field proton acceleration. The physics behind these observations is also investigated.

Concerning proton layer width, it is found that Coulomb explosion plays a very important role in determining proton cut-off energy. We have introduced a model of proton acceleration process integrating the effects of both sheath field and Coulomb explosion to discuss the cut-off energy in detail. We also find that the energy spread becomes narrower with decreasing transverse width, while the proton divergence angle reaches a peak value near $4.0\ \lambda_0$.

https://doi.org/10.1017/S0263034613000517 Published online by Cambridge University Press

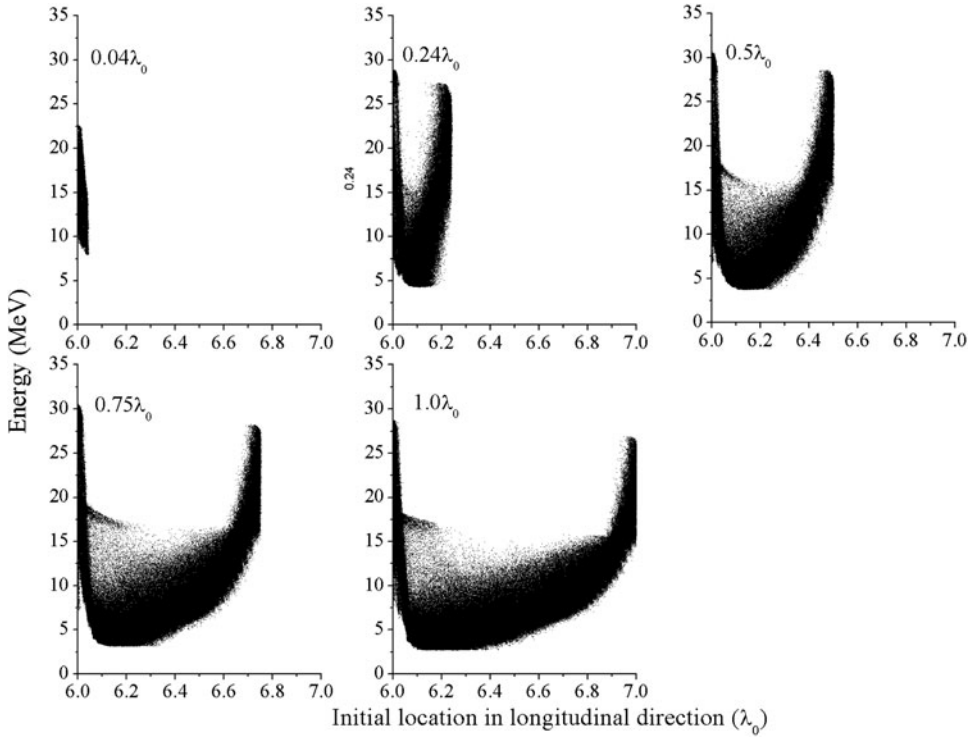

Fig. 8. The relation between proton energy and initial locations in the longitudinal direction. The transverse width of the proton layer is fixed to 5.0 λ_0 and the thickness is changed from 0.04 λ_0 to 1.0 λ_0.

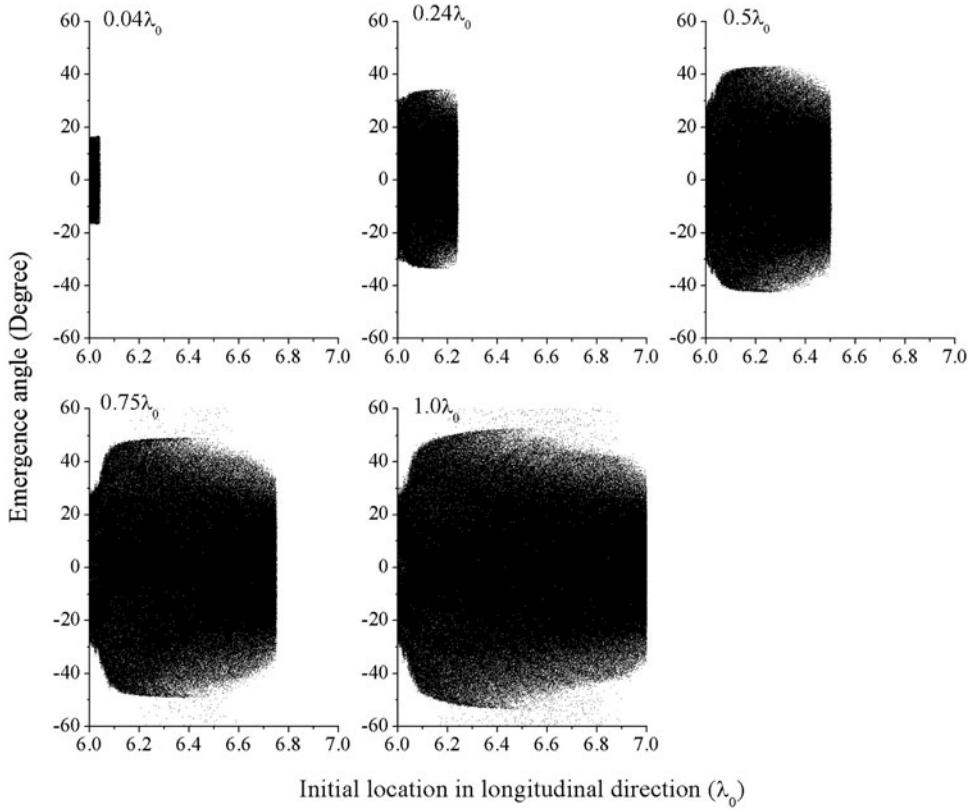

Fig. 9. The relations between proton emergence angle and initial proton locations in the longitudinal direction. The transverse width of the proton layer is fixed to 5.0 λ_0 and the thickness is changed from 0.04 λ_0 to 1.0 λ_0.

https://doi.org/10.1017/S0263034613000517 Published online by Cambridge University Press

We have also found that the proton spectra, cut-off energy and energy spread are also affected by the thickness of the proton layer. We have employed a Coulomb explosion model to explain the trend of cut-off energy of different thickness. There is an optimal thickness, which gives the least energy spread, while the proton divergence angle grows with the proton layer thickness.

ACKNOWLEDGMENTS

This work is supported by the National Natural Science Foundation of China (Grant Nos. 10905009, 11174259, 11175165 and 10975121), the Doctorate Foundation of the Ministry of Education of China (Grant No. 200806141034), and the Fundamental Research Funds for the Central Universities (Grant No. ZYGX2012YB023).

REFERENCES

Andreev, A., Ceccotti, T., Levy, A., Platonov, K. & Martin, Ph. (2010). Divergence of fast ions generated by interaction of intense ultra-high contrast laser pulses with thin foils. *New J. Phys*. **12**, 045007.

Badziak, J., Mishra, G., Gupta, N.K. & Holkundkar, A.R. (2011). Generation of ultraintense proton beams by multi-ps circularly polarized laser pulses for fast ignition-related applications. *Phys. Plasmas* **18**, 035108.

Bartal, T., Foord, M.E., Bellei, C., Key, M.H., Flippo, K.A., Gaillard, S.A., Offermann, D.T., Patel, P.K., Jarrott, L.C., Higginson, D.P., Roth, M., Otten, A., Kraus, D., Stephens, R.B., Mclean, H.S., Giraldez, E.M., Wei, M.S., Gautier, D.C. & Beg, F.N. (2011). Focusing of short-pulse high-intensity laser-accelerated proton beams. *Nat. Phys*. **4**, 139–142.

Brenner, C.M., Green, J.S., Robinson, A.P.L., Carrall, D.C., Dromey, B., Foster, P.S., Kar, S., Li, Y.T., Markey, K., Spindloe, C., Streeter, M.J.V., Tolley, M., Wahlstrom, C.-G., Xu, M.H., Zepf, M., Mckenna, P. & Neely, D. (2011). Dependence of laser accelerated protons on laser energy following the interaction of defocused, intense laser pulses with ultra-thin targets. *Laser Part. Beams* **29**, 345–351.

Burza, M., Gonoskov, A., Genoud, G., Persson, A., Svensson, K., Quinn, M., Mckenna, P., Marklund, M. & Wahlström, C.-G. (2011). Hollow microspheres as targets for staged laser-driven proton acceleration. *New J. Phys*. **13**, 013030.

Cai, H.B., Mima, K., Zhou, W.M., Jozaki, T., Nagatomo, H., Sunahara, A. & Mason, R.J. (2009). Enhancing the number of high-energy electrons deposited to a compressed pellet via double cones in fast ignition. *Phys. Rev. Lett*. **102**, 245001.

Carrié, M., Lefebvre, E., Flaco, A. & Malka, V. (2009). Influence of subpicosecond laser pulse duration on proton acceleration. *Phys. Plasmas* **16**, 053105.

Daido, H., Nishiuchi, M. & Pirozhkov, A.S. (2012). Review of laser-driven ion sources. *Rep. Prog. Phys*. **75**, 056401.

Eliasson, B., Liu, C.S., Shao, X., Sagdeev, R.Z. & Shukla, P.K. (2009). Laser acceleration of monoenergetic protons via a double layer emerging from an ultra-thin foil. *New J. Phys*. **11**, 073006.

Esirkepov, T.Zh., Bulanov, S.V., Nishihara, K., Tajima, T., Pegoraro, F., Khoroshkov, V.S., Mima, K., Daido, H., Kato, Y., Kitagawa, Y., Nagai, K. & Sakabe, S. (2002). Proposed double-layer target for the generation of high-quality laser-accelerated ion beams. *Phy. Rev. Lett*. **89**, 175003/1–4.

Esirkepov, T., Yamagiwa, M. & Tajima, T. (2006). Laser ion-acceleration scaling laws seen in multiparametric particle-in-cell simulations. *Phys. Rev. Lett*. **96**, 105001.

Flacco, A., Sylla, F., Veltcheva, M., Carrié, M., Nuter, R., Lefebvre, E., Batani, D. & Malka, V. (2010). Dependence on pulse duration and foil thickness in high-contrast-laser proton acceleration. *Phys. Rev. E*. **81**, 036405.

Fourkal, E., Velchew, I. & Ma, C.-M. (2005). Coulomb explosion effect and the maximum energy of protons accelerated by high-power lasers. *Phys. Rev. E*. **71**, 036412.

Fuchs, J., Antici, P., D'Humières, E., Lefebvre, E., Borghesi, M., Brambrink, E., Cecchetti, C.A., Kaluza, M., Malka, V., Manclossi, M., Meyroneinc, S., Mora, P., Schreiber, J., Toncian, T., Pepin, H. & Audebert, P. (2006). Laser-driven proton scaling laws and new paths towards energy increase. *Nat. Phys*. **2**, 48–54.

Hegelich, B.M., Albright, B.J., Cobble, J., Flippo, K., Letzring, S., Paffet, M., Ruhl, H., Schreiber, J., Schulze, R. & Fernández, J.C. (2006). Laser acceleration of quasi-monoenergetic MeV ion beams. *Nat. (London)* **439**, 441.

Klimo, O., Psikal, J., Limpouch, J., Proska, J., Novotny, F., Ceccotti, T., Floquet, V. & Kawata, S. (2011). Short pulse laser interaction with micro-structured targets: simulations of laser absorption and ion acceleration. *New J. Phys*. **13**, 053028.

Lefebvre, E., Gremillet, L., Lévy, A., Nuter, R., Antici, P., Carrié, M., Ceccotti, T., Drouin, M., Fuchs, J., Malka, V. & Neely, D. (2010). Proton acceleration by moderately relativistic laser pulses interacting with solid density targets. *New J. Phys*. **12**, 045017.

Li, C.K, Séguin, F.H., Frenje, J.A., Rygg, J.R., Petrasso, R.D., Town, R.P.J., Amendt, P.A., Hatchett, S.P., Landen, O.L., Mackinnon, A.J., Patel, P.K., Smalyuk, V.A., Sangster, T.C. & Knauer, J.P. (2006). Measuring E and B fields in laser-produced plasmas with monoenergetic proton radiography. *Phys. Rev. Lett*. **97**, 135003.

Li, C.K., Séguin, F.H., Frenje, J.A.R., Petrasso, R.D., Amendt, P.A., Town, R.P.J., Landen, O.L., Rygg, J.R., Betti, R., Knauer, J.P., Meyerhofer, D.D., Soures, J.M., Back, C.A., Kilkenny, J.D. & Nikroo, A. (2009). Observations of electromagnetic fields and plasma flow in hohlraums with proton radiography. *Phys. Rev. Lett*. **102**, 205001.

Malka, V., Fritzler, S., Lefebvre, E., D'Humieres, E., Ferrand, R., Grillon, G., Albaret, C., Meyroneinc, S., Chambaret, J.-P., Antonetti, A. & Hulin, D. (2004). Practicability of protontherapy using compact laser systems. *Med. Phys*. **31**, 1587.

Mora, P. (2005). Thin-foil expansion into a vacuum. *Phys. Rev. E* **72**, 056401.

Nodera, Y., Kawata, S., Onuma, N., Limpouch, J., Klimo, O. & Kikuch, T. (2008). Improvement of energy-conversion efficiency from laser to proton beam in a laser-foil interaction. *Phys. Rev. E*. **78**, 046401.

Pae, K.H., Choi, I.W. & Lee, J. (2011). Effect of target composition on proton acceleration by intense laser pulses in the radiation pressure acceleration regime. *Laser Part. Beams* **29**, 11–16.

Passoni, M., Bertagna, L. & Zani, A. (2010). Target normal sheath acceleration: theory, comparison with experiments and future perspectives. *New J. Phys*. **12**, 045012.

Passoni, M. & Lontano, M. (2008). Theory of Light-Ion Acceleration Driven by a Strong Charge Separation. *Phys. Rev. Lett*. **101**, 115001.

Pfotenhauer, S.M., Jäckel, O., Sachtleben, A., Polz, J., Ziegler, W., Schlenvoigt, H.-P., Amthor, K.-U., Kaluza, M.C., Ledingham, K.W.D., Sauerbrey, R., Gibbon, P., Robinson, A.P.L. & Schwoerer, H. (2008). Spectral shaping of laser generated proton beams. *New J. Phys*. **10**, 033034.

Pukhov, A., Kumar, N., Tückmantel, T., Upadhyay, A., Lotov, K., Muggli, P., Khudik, V., Siemon, C. & Shvets, G. (2011). Phase velocity and particle injection in a self-modulated proton-driven plasma wakefield accelerator. *Phys. Rev. Lett*. **107**, 145003.

Robinson, A.P.L., Key, M.H. & Tabak, M. (2012). Focusing of relativistic electrons in dense plasma using a resistivity-gradient-generated magnetic switchyard. *Phys. Rev. Lett*. **108**, 125004.

Roth, M., Cowan, T.E., Key, M.H., Hatchett, S.P., Brown, C., Hatchett, S.P., Brown, C., Fountain, W., Johnson, J., Pennington, D.M., Snavely, R.A., Wilks, S.C., Yasuike, K., Ruhl, H., Pegoraro, F., Bulanov, S.V., Campbell, E.M., Perry, M.D. & Powell, H. (2001). Fast Ignition by Intense Laser-Accelerated Proton Beams. *Phys. Rev. Lett*. **86**, 436.

Sakagami, H., Okada, K., Kaseda, Y., Taguchi, T. & Johzaki, T. (2012). Collisional effects on fast electron generation and transport in fast ignition. *Laser Part. Beams* **30**, 243–248.

Schwoerer, H., Pfotenhauer, S., Jäckl, O., Amthor, K.-U., Liesfeld, B., Ziegler, W., Sauerbrey, R., Ledingham, K.W.D. & Esirkepov, T. (2006). Laser-plasma acceleration of quasi-monoenergetic protons from microstructured targets. *Nat. (London)* **439**, 445.

Ter-Avetisyan, S., Schnürer, M., Nickles, P. V., Sandner, W., Nakamura, T. & Mima, K. (2009). Correlation of spectral, spatial, and angular characteristics of an ultrashort laser driven proton source. *Phys. Plasmas* **16**, 043108.

Wilks, S.C., Langdon, A.B., Cowan, T.E., Roth, M., Singh, M., Hatchett, S., Key, M.H., Pennington, D., MacKinnon, A. & Snavely, R.A. (2001). Energetic proton generation in ultra-intense laser–solid interactions. *Phys. Plasmas* **8**, 542.

Yu, J.Q., Jin, X.L., Zhou, W.M., Li, B. & Gu, Y.Q. (2013). High-order interpolation algorithms for charge conservation in particle-in-cell simulations. *Commun. Comput. Phys*. **13**, 1194–1150.

Yu, J.Q., Zhou, W.M., Cao, L.H., Zhao, Z.Q., Cao, L.F., Shan, L.Q., Liu, D.X., Jin, X.L., Li, B. & Gu, Y.Q. (2012*a*). Enhancement in coupling efficiency from laser to forward hot electrons by conical nanolayered target. *Appl. Phys. Lett*. **100**, 204101.

Yu, J.Q., Zhou, W.M., Jin, X.L., Cao, L.H., Zhao, Z.Q., Hong, W., Li, B. & Gu, Y.Q. (2012*b*). Improvement of proton energy in high-intensity laser-nanobrush target interactions. *Laser Part. Beams* **30**, 307–311.

Zeil, K., Kraft, S.D., Bock, S., Bussmann, M., Cowan, T.E., Kluge, T., Metzkes, J., Richter, T., Sauerbrey, R. & Schramm, U. (2010). The scaling of proton energies in ultrashort pulse laser plasma acceleration. *New J. Phys*. **12**, 045015–16.

Zhang, Z.Y., Shen, B.F., Zhang, X.M., Wang, F.C. & Ji, L.L. (2009). Energetic-ion generation by the combination of laser pressure and Coulomb explosion. *Chinese Physics B*, **18**(12), 5395–06.

Zhou, W.M., Gu, Y.Q., Hong, W., Zhao, Z.Q., Ding, Y.K., Zhang, B.H., Cai, H.B. & Mima, K. (2010). Enhancement of monoenergetic proton beams via cone substrate in high intensity laser pulse-double layer target interactions. *Laser Part. Beams* **28**, 585–590.

https://doi.org/10.1017/S0263034613000517 Published online by Cambridge University Press